HHS Public Access

Author manuscript

Science. Author manuscript; available in PMC 2017 October 30.

Published in final edited form as:

Science. 2016 September 23; 353(6306): . doi:10.1126/science.aaf1420.

A global interaction network maps a wiring diagram of cellular function

A full list of authors and affiliations appears at the end of the article.

Abstract

We generated a global genetic interaction network for *Saccharomyces cerevisiae*, constructing over 23 million double mutants, identifying ~550,000 negative and ~350,000 positive genetic interactions. This comprehensive network maps genetic interactions for essential gene pairs, highlighting essential genes as densely connected hubs. Genetic interaction profiles enabled assembly of a hierarchical model of cell function, including modules corresponding to protein complexes and pathways, biological processes, and cellular compartments. Negative interactions connected functionally related genes, mapped core bioprocesses, and identified pleiotropic genes, whereas positive interactions often mapped general regulatory connections among gene pairs, rather than shared functionality. The global network illustrates how coherent sets of genetic interactions connect protein complex and pathway modules to map a functional wiring diagram of the cell.

Introduction

Genetic interaction networks highlight mechanistic connections between genes and their corresponding pathways (1). Genetic interactions can also determine the relationship between genotype and phenotype (2) and may contribute to the “missing heritability”, or the lack of identified genetic determinants underlying a phenotypic trait, in current genome-wide association studies (3, 4). To explore the general principles of genetic networks, we took a systematic approach to map genetic interactions among gene pairs in the budding yeast, *Saccharomyces cerevisiae*. Synthetic genetic array (SGA) analysis automates the combinatorial construction of defined mutants and enables the quantitative analysis of genetic interactions (1, 5). A positive genetic interaction describes a double mutant that exhibits a fitness that is greater than expected based on the combination of the two corresponding single mutants. Conversely, a negative or synthetic lethal/sick genetic interaction is identified when a double mutant displays a fitness defect that is more extreme than expected (1, 5). Synthetic lethal interactions are of particular interest as they can be harnessed to identify new antibiotic or cancer therapeutic targets (6, 7). In this study, we both expand upon our previous analysis of genetic interactions associated with nonessential

[#]To whom correspondence should be addressed. cmyers@cs.umn.edu brenda.andrews@utoronto.ca, charlie.boone@utoronto.ca.
[≈]Present address: Structural Bioinformatics & Network Biology Lab, Institute for Research in Biomedicine, 08028 Barcelona, Spain
[§]Present address: Yumanity Therapeutics, 790 Memorial Drive, Cambridge, MA, 02139
[¶]Present address: The Francis Crick Institute, Clare Hall Laboratory, South Mimms, Herts. EN6 3LD, United Kingdom
[ϕ]Present address: SciLifeLab, Department of Microbiology, Tumor and Cell Biology. Karolinska Institutet, Solna, Sweden
[∞]Present address: Dept. of Molecular Biology, Princeton University
[*]These authors contributed equally to this work

genes (1) and also characterized genetic interactions involving the majority of essential genes to generate a global yeast genetic interaction network.

A global and quantitative genetic network for yeast

To map genetic interactions between nonessential yeast genes (8), we generated a genome-scale library of *natMX*-marked deletion mutant query strains and crossed them to an array composed of the corresponding *kanMX*-marked deletion mutant collection (9, 10). We also systematically examined genetic interactions between pairs of essential genes (9). To do so, we generated temperature sensitive (TS) mutant alleles, carrying mutations that typically alter coding regions. Our essential gene mutant collection consists of 2,001 array and/or query strains harboring TS alleles corresponding to 868 unique essential genes, with ~600 of genes represented by two or more TS alleles, including strains for ~140 essential genes that were not represented in previous strain collections (11, 12). TS mutants were screened at a semi-permissive temperature where cells were viable but partially compromised for gene function and associated with a reduced growth rate (8). We also constructed a set of essential gene query strains carrying Decreased Abundance of mRNA (DAmP) alleles, which can lead to reduced transcript levels (13); however, only a fraction of DAmP alleles (25%) compromised gene function enough to impact cellular fitness (> 5% fitness defect) and, consequently, most DAmP alleles exhibited fewer interactions compared to TS alleles of essential genes (fig. S1). Thus, TS alleles mediated the majority of the essential gene genetic interactions in our network and the analyses described exclude DAmP alleles, unless otherwise noted.

We constructed three different genetic interaction maps. First, the collection of nonessential deletion mutant query strains was screened against the nonessential deletion mutant array to generate a nonessential x nonessential (NxN) network. Second, query strains carrying TS alleles of essential genes were also screened against the nonessential deletion mutant array to generate an essential x nonessential (ExN) network. Finally, both nonessential deletion mutant and TS query mutant strains were crossed to an array of TS strains of essential genes to generate an expanded ExN network and the first large-scale essential x essential (ExE) genetic network.

Negative and positive genetic interactions were quantified and false negative/positive rates and data reproducibility were determined at defined confidence thresholds (1) from analysis of biological replicates and comparison of interactions for a subset of gene pairs represented on both mutant arrays (fig. S2)(8). A global genetic interaction network resulting from the combination of the NxN, ExN, and ExE networks was generated from analysis of ~23 million double mutants encompassing 5,416 different genes. In total, we identified nearly 1 million genetic interactions, corresponding to ~550,000 negative and ~350,000 positive genetic interactions, including ~120,000 interactions between pairs of essential genes (fig. S3). The current global network involves ~90% of all yeast genes as query and/or array mutants and is accessible from http://thecellmap.org/costanzo2016/. We note that experiments and analyses described here were from a representative subset (> 80%) of the complete dataset (Data Files S1–S3).

A functional map of a cell

The genetic interaction profile of a particular gene is composed of its specific set of negative and positive genetic interactions. Genes belonging to similar biological processes tend to share common genetic interactions, and genes encoding proteins that function together within the same pathway or complex display similar genetic interaction profiles (fig. S4)(1). Thus, genetic interaction profiles provide a quantitative measurement of functional similarity, and similarity networks generated from the large-scale mapping correlated genetic interaction profiles organizes genes into clusters that highlight biological processes (1). We visualized networks of genetic profile similarity (Data File S3) between essential genes (Fig. 1A, Essential Similarity Network), nonessential genes (Fig. 1B, Nonessential Similarity Network), and a combined global similarity network (Fig. 1C, Global Similarity Network). Nodes in the similarity networks represent genes whereas edges connect gene pairs that share similar genetic interaction profiles (8).

When evaluated at the same Pearson correlation coefficient (PCC) threshold, the essential gene similarity network (Fig. 1A) was more than 25-fold more densely connected compared to the corresponding nonessential network (Fig. 1B). For example, at PCC ≥ 0.2, 3.12% of all tested gene pairs were connected in the ExE similarity network, whereas 0.12% of all tested gene pairs were connected in the NxN similarity network. Moreover, genes on the essential gene similarity network often showed a stronger functional relationship, because genes that encode members of the same essential protein complex exhibited significantly higher interaction profile similarity than gene pairs belonging to the same nonessential complex (fig. S5). By evaluating the predictive power of both essential and nonessential genetic interaction profiles (8), we found that essential gene interaction profiles provided higher accuracy gene function predictions across a diverse set of biological processes (14), and this increased accuracy was correlated with the fraction of essential genes annotated to specific bioprocesses (fig. S6; Data File S4). Nevertheless, interactions involving either essential or nonessential genes can predict function. For example, interactions involving nonessential genes were more predictive of vacuolar transport, peroxisome, and mitochondrial function, whereas interactions involving essential genes were more informative for predicting chromosome segregation, mRNA splicing, and proteolysis functions. Interestingly, functional predictions for essential genes could also be derived from interactions with nonessential genes and vice versa. Nevertheless, optimal functional prediction performance was achieved with a global similarity network that combined the majority of all nonessential and essential protein coding genes in the *S. cerevisiae* genome.

To functionally annotate the global genetic profile similarity maps (Fig. 1A–C), we applied Spatial Analysis of Functional Enrichment (SAFE), which identifies dense network regions associated with specific functional attributes (15). Implementing SAFE with 4373 biological process terms from Gene Ontology (GO)(14), we detected gene clusters in each similarity network that were enriched for unique sets of related GO terms (Fig. 1D–F; Data File S5). Gene clusters enriched for GO terms related to cell polarity, protein degradation, and rRNA processing, were specifically detected in the essential gene similarity network (Fig. 1D), whereas the nonessential gene similarity network identified clusters enriched for mitochondrial and peroxisomal functions (Fig. 1E). The global similarity network provided

a more organized and functionally comprehensive view of cellular function, emphasizing the importance of mapping genetic interactions that involve both nonessential and essential genes (Fig. 1F). SAFE identified 487 significantly enriched GO bioprocess terms that mapped to 17 unique network regions and covered 1343 genes on the global network (Fig. 1F). The subsets of enriched GO bioprocess terms associated with each densely connected network region in turn revealed genes involved in core cellular functions and defined an informative subset of GO bioprocess terms associated with these functions (Data File S5).

Genetic profile similarities map a hierarchy of gene and cellular function

The relative positioning of biological process clusters appeared to reflect shared functionality because distinct, but related processes such as DNA Replication & Repair and Mitosis & Chromosome Segregation, were positioned next to each other in the global similarity network (Fig. 1F). To explore this functional organization more rigorously, we considered only those genes with at least one highly similar gene partner, resulting in a set of 515 nonessential and 421 essential array mutants (8). We then applied an unsupervised clustering approach to construct a genetic interaction-based hierarchy for this subset of genes. The base of the resultant hierarchy was composed of numerous, small clusters of genes with highly similar genetic interaction profiles, whereas the top of the hierarchy was composed of a small set of larger clusters of genes with lower profile similarity (Figs. 2A, S7; Data File S6).

To examine functional relationships between clusters identified at different hierarchical levels, we assessed whether distinct “sibling” clusters, resolved at one level of the hierarchy and combined together at a higher level to generate a unique and larger “parent” cluster, shared enrichment for the same annotations from a particular functional standard (8). Indeed, sibling clusters identified at a relatively high level of profile similarity (e.g. PCC > 0.4), which often corresponded to distinct protein complexes, shared enrichment for the same GO biological process annotations (Data File S6). For example, five sibling clusters with distinct pathway/complex annotations, including the homologous DNA repair pathway and the ORC (Origin Recognition Complex), combined together into a single parent cluster, and all these siblings are enriched for GO biological process terms such as “DNA repair”, “DNA metabolic process”, and “Response to DNA damage stimulus”, which reflects a general role shared by the collective gene set in the regulation of DNA synthesis and repair (Data File S6).

However, sibling clusters detected at an intermediate range of profile similarity (0.2 < PCC < 0.4), which combined into a relatively smaller set of larger parent clusters at a lower range of profile similarity (0.05 < PCC < 0.2), did not share enrichment for the same GO biological process, pathways or protein complex annotations. Instead, these clusters were enriched for genes whose products function in the same cell compartment (Figs. 2A, S7; Data File S6). For example, one of the ten parent clusters formed near the top of the hierarchy was comprised of six sibling clusters, and, although each individual sibling cluster was enriched for unique GO biological process terms including “Chromosome Segregation”, “Transcription from RNA Polymerase II Promoter” or “DNA Repair”, none of the sibling clusters were enriched for the same GO biological process terms. Instead, all ten sibling

clusters were enriched for gene products that exhibit nuclear localization patterns (Data File S6). As observed previously (16), this indicates that novel functional organization is embedded within large-scale, unbiased datasets, which may not be captured completely by functional standards, including GO as it is currently organized (14). Thus, a global genetic interaction network, created on the basis of a single fitness phenotype, quantifies functional relatedness to organize genes into modules corresponding to protein complexes and pathways, which combine to define specific biological processes which, in turn, group together into larger modules representing specific cellular compartments, thereby revealing a hierarchical model of cell function.

The functional hierarchy revealed by genetic interaction profiles can also be visualized on the global similarity network (Fig. 2B). Applying SAFE with a protein localization standard (17), we detected 14 network regions enriched for genes whose products localize to 11 different subcellular compartments (Fig. 2B, Localization). For example, bioprocess clusters such as DNA synthesis, Mitosis, Nuclear Transport and Transcription (Fig. 2B, GO BP; Data File S5) combined into a single module encompassing genes localized to the cell nucleus (Fig. 2B, Localization). At a higher level of functional resolution, SAFE identified 28 gene clusters corresponding to 123 specific protein complexes (Fig 2B, Complexes; Data File S5). Functional relationships between protein complexes were also resolved in greater detail by extracting biological process-enriched clusters from the global network and visualizing them in isolation (Fig. 3; Data File S5).

Quantifying genetic pleiotropy

The ability of an organism to tolerate environmental and genetic variation may be dependent on phenotypic capacitors, a class of genes whose inactivation may increase phenotypic variation among genetically diverse individuals in a population (18). Hsp90, the canonical capacitor, is a molecular chaperone controlling numerous signaling pathways and thus is considered a multi-functional or pleiotropic gene (18). Identifying other pleiotropic genes may uncover novel capacitors and provide insight into the genetic basis of phenotypic robustness.

We expect that a pleiotropic gene involved in diverse functions should show a genetic interaction profile that partially overlaps with genes representative of its functional spectrum. To quantify pleiotropy, we focused on genes with a high degree of negative genetic interactions and developed a pleiotropy score that measured the functional breadth of genetic interaction profiles associated with these genes (8). Genes encoding Hsp90 (*hsc82*Δ*hsp82-5001* TS double mutant query strain; Data File S1), *IRA2*, a negative regulator of RAS signaling, and *RSP5*, an E3 ubiquitin ligase, ranked among the most highly pleiotropic genes observed (Data File S7). Other highly pleiotropic genes (top 30% pleiotropy scores) included those with proteostasis or signaling roles, as well as select genes with roles in fundamental cellular functions, such as translation, RNA processing, vesicle trafficking, lipid metabolism, and coenzyme-A biosynthesis (Fig. 4A). Because they share genetic interactions with many functionally diverse genes, high pleiotropy genes tended not to belong to densely connected network clusters, but rather were more often positioned outside the functionally enriched clusters, scattered in the sparser regions of the global

network (Fig. 4A). In contrast, high degree but low pleiotropy genes (lowest 30% pleiotropy scores), which are functionally specific, overlapped more often with densely connected regions of the global similarity network ($P < 10^{-5}$; Gene Set Enrichment Analysis)(8)

Predicting novel gene function

The location of numerous previously uncharacterized genes either within or in close proximity to functionally enriched regions of the genetic profile similarity network allows us to predict functions for these genes (Fig. 4B)(8). Notably, while most essential genes are relatively well studied, our network uncovered a role for a previously uncharacterized essential gene, *YJR141W*, which we named *IPA1* (Important for cleavage and PolyAdenylation), in the highly conserved process of mRNA 3′-end processing and polyadenylation. *IPA1* shares many genetic interactions in common with genes encoding members of the Cleavage/Polyadenylation factor (CPF) and Cleavage Factor IA (CF IA) protein complexes (Fig. 4B, C), which along with *HRP1*, are essential for mRNA 3′ end processing (19). We also found that Ipa1 physically interacted with CPF complex members, Mpe1 and Ysh1 (Data File S8)(8) further supporting a role for *IPA1* in this process. Indeed, as shown previously for TS mutants in components of CF IA and CPF complexes (20), such as *pcf11* and *cft2* TS mutants, an *ipa1* TS mutant was impaired for *in vitro* mRNA cleavage and polyadenylation (fig. S8) and showed widespread defects in mRNA processing accuracy and efficiency with a significant bias towards the use of downstream polyadenylation sites ($P < 2 \times 10^{-16}$, Wilcoxon rank sum; Figs. 4D; S8)(8).

Six poorly characterized genes, *MTC2, MTC4, MTC6, CSF1, DLT1,* and *YPR153W* localized in the vicinity of the cell polarity and morphogenesis cluster on the global network (Fig. 4B) and displayed highly similar genetic interaction profiles suggesting that they work together as a novel functional module (Fig. 4E). Interestingly, all of these genes were identified as important for growth in high-pressure and cold environments (21). Thus, we called this module the MTC pathway and named *YPR153w* as *MAY24* (genetic interaction profile similarity to MTC Annotated Yeast genes *MTC2* and *MTC4*). *MTC2*, *MTC4*, and *MTC6* mutants were previously shown to enhance the mutant phenotype associated with perturbation of *CDC13*, which controls the maintenance of telomere capping (22). MTC pathway genes showed strong negative interactions with protein trafficking genes, as well as aromatic amino acid biosynthesis genes, *ARO1* and *ARO2* (Figs. 4F, S9). Because pathway components often share phenotypes with their target genes, a genetic interaction profile that contains members of a particular pathway may also identify potential targets of the same pathway. For example, the *ARO1* genetic interaction profile revealed strong negative interactions with genes involved in amino acid metabolism, the entire MTC pathway and the aromatic amino acid transporters, *BAP2* and *TAT1* (Figs. 4G, S9), suggesting that the MTC pathway may control amino acid metabolism or affect trafficking of Bap2 and Tat1 permeases. Indeed, mutations of MTC pathway genes resulted in Bap2 mislocalization (Figs. 4H, S9) and a defect in phenylalanine uptake, resembling that of strains deleted for genes encoding amino acid transporters, including *BAP2*, *TAT1*, and *GAP1* (Fig. 4I)(8). Furthermore, unbiased metabolomics analysis revealed that the MTC pathway mutants exhibited elevated levels of kyurenine biosynthetic pathway metabolites, including NAD+ (Fig. 4J)(8). Previous studies showed that defects in kyurenine biosynthesis suppressed

cdc13-1 TS mutants, suggesting that elevated NAD+ levels inhibit telomere capping (23). Thus, the global genetic interaction network traced novel functional connections whereby defects in MTC pathway-dependent protein trafficking alter aromatic amino acid homeostasis, which appears to modulate steady state levels of kyurenine biosynthetic pathway metabolites, linking cell polarity to telomere capping through altered NAD+ levels.

Genetic interaction network connectivity

Genetic interaction profiles connect a particular gene to other genes through both negative and positive interactions. Although the average gene participated in ~100 negative interactions (2% of genes tested) and ~65 positive interactions (1% of genes tested), when assessed at an intermediate confidence threshold (8), a wide range of connectivity exists in the genetic interaction network (fig. S10; Data File S9). For example, the 10% most connected genes (i.e. high interaction degree genes or hub genes) in the genetic interaction network participated in 3.5-fold more genetic interactions than the average gene. More specifically, negative interaction hubs had an average degree of 340 negative interactions and the average positive interaction hub displayed 200 positive interactions. In general, essential genes participated in ~5-fold more negative and positive interactions than nonessential genes, confirming previous estimates (Fig. 5A)(24).

As observed previously (1), fitness defects associated with both deletion alleles of nonessential genes and TS alleles of essential genes were highly correlated with the degree of genetic interaction (figs. S11–S12; Table S1; Data File S10). In the global network, genetic interaction hubs participated in numerous chemical-genetic interactions and tended to encode conserved, multifunctional, highly expressed and abundant proteins that exhibit many physical interactions (Data File S9; Table S1). Genes encoding proteins involved in specific biochemical functions, or those that contain specific functional domains, such as an SH3 (SRC Homology 3) protein-protein interaction domain, were also associated with a higher number of genetic interactions (figs. S13, S14). In the nonessential genetic interaction network (NxN), negative and positive interaction hubs were enriched for biological processes including chromatin organization, transcription and vesicle trafficking (Data File S11). In the essential genetic network (ExE), negative interaction hubs were relatively uniformly distributed across all bioprocesses, whereas positive interaction hubs were specifically enriched for proteostasis-related bioprocesses (Data File S11).

Genes that exhibited relatively few genetic interactions were also associated with specific features (figs. S11–S14; Table S2; Data File S10). For example, ABC transporters, which belong to functionally redundant gene families and thus are extensively buffered, exhibited fewer genetic interactions (figs. S11–S14; Table S2). Interestingly, genes with lowest interaction degree (lowest 20%; Data File S9) were often associated with more deleterious single nucleotide polymorphisms (SNPs), exhibited a higher dN/dS ratio, and displayed high expression variance across different genetic backgrounds and environments. This suggests that these genes are under reduced evolutionary constraints and subject to condition-specific regulation (Table S2; figs. S11–S12). Approximately 1000 genes (~20%), the majority of which are nonessential genes, displayed few genetic interactions and had profiles that generally displayed a relatively low level of functional information, suggesting that the

connectivity for some genes will only be revealed under different environmental or genetic conditions. The functional, physiological and evolutionary properties associated with genetic interaction frequency should predict genetic network connectivity and candidate genes that may serve as important genetic modifiers in other organisms, including humans (25).

Negative and positive genetic interactions of essential and nonessential genes

The global genetic interaction network, encompassing the majority of both nonessential and essential genes, enabled a comprehensive comparative analysis with other functional information (8). Both nonessential and essential genetic interactions were predictive of functionally related gene pairs (Figs. 5B, C, S15). In particular, negative interactions among essential genes showed a striking overlap with protein-protein interactions (Figs. 5C, S15). For example, 50% of essential gene pairs whose products physically interact also share a negative interaction, representing a ~10-fold enrichment for negative interactions among essential genes displaying protein-protein interactions. Similarly, 63% of gene pairs annotated to the same essential protein complex were connected by a negative genetic interaction, representing a ~15-fold enrichment for negative interactions among co-complexed essential gene pairs. In fact, individual negative interactions were as informative as genetic interaction profile similarity for predicting membership to the same essential pathway or complex, a property that does not hold for nonessential genes (fig. S16). This observation highlights the reduced ability of a cell to tolerate multiple partial loss-of-function mutations in the same essential pathway or complex (Figs. 5C, S15).

Consistent with previous observations (1), positive genetic interactions between nonessential genes also overlapped with protein-protein interactions, albeit to a lesser extent (0.5%, 3.7-fold enrichment; Figs. 5C, S15). This reflects that simultaneous perturbation of two genes encoding members of the same nonessential protein complex often show a fitness defect resembling the corresponding single mutants. In contrast, we did not detect any overlap between essential gene positive interactions and other molecular or functional relationships, including physical interactions (Figs. 5B, C, S15). The lack of a functional signal could not be explained by differences in data quality because replicate analysis confirmed that SGA-derived positive and negative interactions showed similar levels of reproducibility (fig. S2). Furthermore, members of the same essential protein complex or different alleles of the same essential gene often showed similar positive interaction profiles (fig. S17). Thus, while negative interactions identified clear functional relationships between genes, positive interactions amongst partial loss-of function alleles of essential genes represent a different type of relationship that is not captured by other large-scale datasets or functional standards.

Functional distribution of genetic interactions within and between bioprocesses

We further examined the functional distribution of genetic interactions, through the enrichment for negative and positive interactions within and between biological processes (Fig. 1F; Data File S6)(8). Negative genetic interactions were significantly enriched ($P <$

0.05, hypergeometric) among genes belonging to the same biological process in both the nonessential (NxN) and essential (ExE) genetic interaction networks (Fig. 5D, on-diagonal). Negative interactions were also enriched between deletion alleles of nonessential genes in different biological processes (Fig. 5D, off-diagonal). In contrast, negative interactions between TS alleles of essential genes, despite higher abundance (Fig. 5A), were biased towards gene pairs in the same biological processes (Fig. 5D, on-diagonal) and were rarely enriched between genes involved in different biological processes (Fig. 5D, off-diagonal). Although these trends could reflect the different genetic perturbations used to interrogate nonessential and essential genes**,** negative interactions among essential genes highlight a core set of cellular bioprocesses and nonessential genes appear to mediate connections between these bioprocesses.

While nonessential genes involved in the same biological process were modestly enriched for positive interactions, we failed to observe a similar enrichment for positive interactions among functionally related essential genes (Fig. 5D, on diagonal). Instead, positive interactions tended to connect essential genes with roles in highly distinct biological processes. In particular, we observed significant enrichment for positive interactions that connected essential genes with nuclear-related functions to essential genes required for vesicle traffic-dependent functions (Figs. 5D, S17).

The architecture of negative interactions within the genetic network hierarchy

To explore the functional distribution of genetic interactions in more detail, we examined where genetic interactions occurred within the genetic network hierarchy of gene function derived from profile similarities. Specifically, we assessed how frequently negative interactions connected a pair of genes belonging to the same cluster within the hierarchy of genetic interaction profiles (Fig. 2A), and we examined clusters corresponding to either a cellular compartment, biological process, or pathway/complex (Fig. 6A)(8). The density (i.e. number of observed interactions relative to the total number of gene pairs screened) of negative interactions, among genes in both the nonessential (NxN) and essential (ExE) genetic interaction networks, increased with the functional specificity of a given cluster. Accordingly, genes within a cluster enriched for specific pathways or complexes were connected by negative interactions more often than genes in the same biological process-enriched cluster, which in turn, were more frequently connected by negative interactions than genes belonging to a cluster enriched for a specific cell compartment (Fig. 6B). For example, essential genes that fall into a cluster within the set that was enriched for complexes/pathways (PCC 0.4–0.8) were connected by a negative interaction with a relatively high density (60–90%), but they were rarely connected by a positive interaction. In total, 43% of nonessential and 56% of essential genes pairs connected by negative interactions shared some degree of functional relatedness (Fig. 6C).

The magnitude of a given negative interaction was also associated with the extent of functional similarity shared between genes (Fig. 6D). For both nonessential and essential genetic interactions, stronger interactions tended to connect genes with closer functional

relationships (Fig. 6D). Thus, on the basis of the strength of negative genetic interaction, we can predict if two genes share an intimate relationship and possibly function in the same pathway or complex. For example, members of the conserved ER Membrane protein Complex, including *EMC1*, *EMC2*, and *EMC6*, which play a role in phospholipid transfer from the ER to mitochondria to facilitate phosphatidylethanolamine biosynthesis (26), showed strong negative genetic interactions (genetic interaction score < −0.65) with a previously uncharacterized essential gene, *YNL181w*, suggesting a role for this gene in lipid metabolism. Indeed, *YNL181w* encodes a putative oxidoreductase that localizes to the ER (27) and, consistent with defective membrane function, *ynl181w* hypomorphic mutants showed altered sensitivities to numerous bioactive compounds (fig. S18)(8). We named this gene *PBR1* (Potentiates Bioactive compound Response) to highlight its role in xenobiotic sensitivity.

The architecture of positive interactions within the genetic network hierarchy

Positive interactions among nonessential genes exhibited similar albeit weaker trends, where the density of interactions increased gradually with the functional specificity of hierarchy-derived clusters (Fig. 6B) and the magnitude of nonessential positive interactions was predictive of nonessential pathway or complex membership (Fig. 6D). In contrast, the density of positive interactions detected in the essential network was not related to functional specificity. In fact, the most distantly related essential gene pairs were more frequently connected by positive interactions than gene pairs mapping to the same biological process-level clusters (Fig. 6B). The majority of positive interacting gene pairs in both the essential (ExE, 78%) and nonessential (NxN, 75%) genetic interaction networks occurred between distantly connected genes whose products appeared to function in different cell compartments (Fig. 6C). Moreover, we did not observe a relationship between functional similarity and the magnitude of positive interactions between essential gene pairs (Fig. 6D). Thus, positive interactions between essential genes generally appear to reflect more functionally distant relationships.

Genetic interactions within and between protein complexes

Consistent with previous findings (1, 5, 28, 29), we found that protein complexes exhibited highly organized patterns of genetic interactions. For example, many protein complexes tested (60/141, 43%) were enriched ($P < 0.01$, hypergeometric) for genetic interactions within the set of protein complex encoding genes and were biased for a single type of interaction, either negative or positive, highlighting the coherent nature of genetic interactions shared among genes encoding members of the same complex. The type of interaction observed within protein complexes depended on essentiality. For example, complexes composed primarily of nonessential genes (> 75% nonessential genes; Data File S12) were more often enriched for positive (21%, 20/97 complexes) compared to negative (5%, 5/97 complexes) interactions among their members (Fig. 7A; Data File S13). In contrast, most essential protein complexes (> 75% essential genes; Data File S12) were enriched for negative interactions among their members (82%; 35/44 complexes). Notably,

none of the essential complexes in our dataset were enriched for positive interactions (Fig. 7A; Data File S13).

The genetic interactions occurring within protein complexes can even resolve the structural organization of large, multi-subunit complexes. For example, while proteasome genes tend to be connected by negative genetic interactions, genes encoding components of the same subunit (e.g. within 19S or within 20S) interact more frequently with one another than genes belonging to different subunits (between 19S and 20S; fig. S19). Phenotypic differences between proteasome subunits were also supported by chemical-genetic interactions observed in yeast (fig. S19)(30) as well as in *Drosophila melanogaster* cultured cells (fig. S20; Data File S14)(8), suggesting that the topology of genetic networks connecting genes within protein complexes by uniform sets of genetic interactions is conserved in higher eukaryotes.

We also examined the topology of genetic interactions occurring between protein complexes and found a large number of complex-complex pairs that were both enriched for genetic interactions ($P < 0.001$, hypergeometric) and strongly biased towards either negative or positive interactions (8). More complex-complex pairs were connected by coherent sets of negative than positive interactions (Fig. 7B; Data File S13). For example, 4% of all nonessential pairs of protein complexes tested (293/6899) were connected by negative interactions, whereas positive interactions connected less than 2% of nonessential complexes (130/6899). Similarly, 5% (74/1597) of all essential complex pairs in our dataset were connected by negative interactions, whereas less than 2% (29/1597) of essential protein complex pairs shared positive interactions (Fig. 7B; Data File S13). Nonetheless, we observed hundreds of instances of both coherent negative (470) and positive (192) interactions connecting pairs of essential and nonessential complexes emphasizing the highly organized topology of genetic interaction networks (Fig. 7B; Data File S13).

Functional wiring diagrams of protein complexes

Extracting all genetic interactions for specific protein complexes generated functional wiring diagrams that revealed the set of genes, pathways, and bioprocesses, modulated by mutation of a particular complex (Fig. 8A, B). For example, coherent sets of negative interactions involving the ORC, which specifies sites of initiation of DNA replication throughout the genome (31), linked functionally related complexes, including the MCM (Mini-Chromosome Maintenance) and the GINS (Go, Ichi, Ni, San) complexes (Fig. 8A), both of which participate in the initiation of DNA replication (32, 33). In another example, negative interactions associated with the 19S proteasome highlighted diverse functions that are particularly important when proteasome activity is compromised (Fig. 8B), including interactions with genes encoding the APC (Anaphase Promoting Complex), which targets cell cycle proteins for degradation to promote exit from mitosis (34). Interestingly, essential genes that showed negative interactions with the proteasome were enriched for multidomain proteins, suggesting that TS alleles may perturb folding of more complex proteins resulting in a greater dependence on proteasome activity in mutants (fig. S21).

Positive interactions among essential genes reflect general regulatory mechanisms

Protein complexes involved in proteostasis, including several chaperones and the proteasome, exhibited among the strongest enrichment for positive genetic interactions, especially in the essential gene network (Figs. 8C, S22; Data File S15). Positive genetic interactions connected the proteasome and other proteostasis-related complexes to genes involved in various functions, including vesicle trafficking and transcription (Figs. 5D, 8B, S23). Because the proteasome plays a direct role in controlling protein turnover, we hypothesized that a subset of its positive interactions may reflect genetic suppression through the stabilization of a mutant protein (35). Indeed, we further tested a subset of these positive interactions (8) and, based on this analysis, we estimated that ~30% of proteasome positive interactions represent genetic suppression, where a fitness defect associated with a hypomorphic TS allele of an essential gene is suppressed by a second mutation in a proteasome encoding gene (Table S3; fig. S24; Data File S16). In total, 16% of positive interactions with essential genes appear to be associated with proteostasis. In a similar regulatory relationship, positive interactions were also enriched between genes involved in mRNA decay and essential gene DAmP alleles (13), which often affect mRNA stability via disruption of their 3′ UTR (fig. S24).

Interestingly, a subset of protein complexes, in addition to being enriched for positive interactions (Fig. 8C), also exhibited more positive interactions compared to negative interactions with essential genes (Fig. 8D; Data File S15). The positive interactions of these biased complexes, were also more functionally diverse compared to their negative interactions. For example, ORC subunits were connected by coherent sets of positive interactions to genes with roles in several different functions including members of the ER-associated Translocon complex (Fig. 8A). The ORC-Translocon connection reflects enrichment for cross-compartment positive interactions observed between genes encoding essential, nuclear and vesicle traffic-dependent functions (Fig. 5D).

Protein complexes with a positive interaction bias tend to be involved in cell cycle progression and their disruption often leads to a cell cycle delay or arrest phenotype (Figs. 8D, S22). A cell cycle delay may result when a mutation activates a checkpoint pathway which slows cell cycle progression, allowing the cell to correct an otherwise rate-limiting defect to mask the phenotypic effect normally associated with a second mutation (36). Thus, an ORC-dependent S-phase cell cycle delay may mask growth defects associated with perturbation of genes required for polarized secretion during budding, thereby resulting in positive interactions. Protein complexes biased for positive interactions with essential genes also exhibited many negative interactions with checkpoint genes ($P < 4\times10^{-56}$, Fisher's exact test; fig. S22), suggesting that cell viability depends on an active checkpoint response in the absence of these complexes. Genes with cell cycle progression-related roles accounted for 30% of essential gene positive interactions, which combined with genes involved in proteostasis, explain 46% of the positive interactions among essential genes.

Discussion

A global network based on genetic interaction profile similarity resolves a hierarchy of modules, enriched for sets of genes within specific pathways and protein complexes, biological processes, or subcellular compartments. In the context of this functional organization, coherent sets of negative and positive genetic interactions connect both within and between the highly resolved complex and pathway modules to map a functional wiring diagram of the cell.

Our comprehensive analysis of genetic interactions among essential genes revealed several illuminating principles. First, consistent with the results of our previous smaller scale surveys (1, 24), essential genes are major hubs and form the basic scaffold of the global genetic interaction network. Second, the extreme negative or synthetic lethal interactions among essential genes often occur between genes within the same protein complex, or between genes in different protein complexes but within the same biological process or subcellular compartment, properties that may prove useful for predicting genetic interactions in other systems. Third, positive genetic interactions between two essential genes typically do not reflect shared function, but rather often occur between genes in distant cellular compartments and reflect more general regulatory connections associated with a cell cycle delay or proteostasis.

An important property associated with the global network is the potential for digenic interactions to compound the phenotypes associated with single gene mutations. While only ~1000 genes in the yeast genome are individually essential in standard growth conditions and cause lethality when mutated (9, 10), we showed that hundreds of thousands of mutant gene pair combinations result in a negative interaction in the global genetic interaction network, including an extreme set of ~10,000 synthetic lethal interactions between nonessential gene pairs (8). In other words, we discovered a genetic background in which an additional ~3,300 genes are essential for viability (8). Despite the power of this approach for uncovering growth dependencies, ~1000 of the 5,400 yeast genes we examined showed relatively few genetic interactions and remain sparsely connected. Our global genetic network was mapped under a particular condition in a specific genetic background, and we anticipate that changing these two key factors may reveal new interactions for many of the sparsely connected genes (37). Ultimately, broad mapping of both core and condition-specific genetic interactions promises to accelerate the field of synthetic biology, providing a rational understanding of the requirements for the design of minimal genomes (38).

It is also important to consider other types of genetic interactions, beyond those associated with loss-of-function mutations in haploid cells. Our analysis revealed that relatively severe deletion alleles of nonessential genes or TS alleles of essential genes often show extensive digenic interaction profiles. However, it is possible that the more subtle mutations associated with natural genetic variation may require higher order combinations, involving more than two genes, to modulate phenotype and influence heritability extensively (39). One interesting case involves duplicated genes with overlapping function, which often are buffered more extensively, such that more complex triple mutant analysis will be required to reveal their genetic interaction profiles (1, 40). We must also understand the general

principles associated with genetic networks involving gain-of-function alleles and more complex genetic interactions that can occur in diploid and polyploid organisms (41), across a variety of different cell types, within whole animals (42–44), or between hosts and their symbiotic organisms (45).

Because negative genetic interactions are highly ordered and often occur as coherent sets, (e.g. predominantly negative genetic interactions connecting genes within a protein complex or between two different protein complexes), many different pairs of mutations may lead to same terminal synthetic lethal/sick phenotype. We suspect that this network topology is important when considering the genotype to phenotype problem in human genetics. Since biological systems are built upon sets of conserved genes whose products participate in functional modules, it is reasonable to expect that the general topology of genetic networks will also be conserved (25). As observed for the complex-complex connections on the global yeast genetic network, mutations in many different pairs of genes may lead to the same phenotype, such as a disease state, in humans. This property of genetic networks means that scanning disease cohorts for genetic variation that corresponds to coherent sets of mutations that connect genes within or between protein complexes and pathways (e.g. see functional wiring diagrams for the ORC the 19S proteasome, Fig. 8) may reveal genetic networks underlying diseases.

The regulatory mechanisms associated with positive genetic interactions among essential genes, which include genetic suppression interactions, are also potentially relevant to human genetics because they may inspire novel therapeutic approaches and elucidate mechanisms of heritability(46, 47). Notably, mutations that compromise the cellular proteostasis network often suppressed TS alleles of essential genes (Table S3; Data File S16). It is possible that, similar to yeast, certain variants of the human proteasome also suppress the detrimental effects of genetic variation associated with numerous other genes, and their corresponding complexes and pathways, within the human genome. While the genes encoding the proteasome are essential in human cells, and severe mutations in these genes may cause disease (48), genetic variation that modulates proteasome function subtly may have the potential to be disease protective.

It is clear that the digenic interactions we have mapped in yeast can be conserved in different yeast species over hundreds of millions of years of evolution (49, 50). Likewise, conservation of genetic interactions from yeast to human cells has been observed (51, 52), particularly within fundamental bioprocesses like DNA synthesis and repair and chromosome segregation, which is particularly relevant for the identification of targets for novel synthetic lethal cancer therapies (53, 54). However, the general extent and breadth of network conservation remains largely unexplored. Importantly, genome-scale application of CRISPR-Cas9 genome editing approaches offer the potential to map global genetic interaction networks in human cells (55–57). We suspect that the general principles of the global yeast genetic network described here will be highly relevant for both the efficient mapping and interpretation of analogous networks in a variety of different cells and organisms.

Methods Summary

Methods for construction of yeast double mutant strains, identification and measurement of genetic interactions as well as all analyses pertaining to genetic interaction profiles, negative and positive interactions are described in detail in the supplementary materials. General information about our methods, accompanied by specific references to the supplementary materials, is included throughout the text.

Supplementary Material

Refer to Web version on PubMed Central for supplementary material.

Authors

Michael Costanzo[1,*], Benjamin VanderSluis[2,3,*], Elizabeth N. Koch[2,*], Anastasia Baryshnikova[4,*], Carles Pons[2,*,≈], Guihong Tan[1,*], Wen Wang[2], Matej Usaj[1], Julia Hanchard[1,5], Susan D. Lee[6], Vicent Pelechano[7,ϕ], Erin B. Styles[1,5], Maximilian Billmann[8], Jolanda van Leeuwen[1], Nydia van Dyk[1], Zhen-Yuan Lin[9], Elena Kuzmin[1,5], Justin Nelson[2,10], Jeff S. Piotrowski[1,11,§], Tharan Srikumar[12,∞], Sondra Bahr[1], Yiqun Chen[1], Raamesh Deshpande[2], Christoph F. Kurat[1,¶], Sheena C. Li[1,11], Zhijian Li[1], Mojca Mattiazzi Usaj[1], Hiroki Okada[13], Natasha Pascoe[1,5], Bryan-Joseph San Luis[1], Sara Sharifpoor[1], Emira Shuteriqi[1], Scott W. Simpkins[2,10], Jamie Snider[1], Harsha Garadi Suresh[1], Yizhao Tan[1], Hongwei Zhu[1], Noel Malod-Dognin[14], Vuk Janjic[15], Natasa Przulj[14,16], Olga G. Troyanskaya[3,4], Igor Stagljar[1,5,17], Tian Xia[2,18], Yoshikazu Ohya[13], Anne-Claude Gingras[5,9], Brian Raught[12], Michael Boutros[8], Lars M. Steinmetz[7,19], Claire L. Moore[6], Adam P. Rosebrock[1,5], Amy A. Caudy[1,5], Chad L. Myers[2,10,#], Brenda Andrews[1,5,#], and Charles Boone[1,5,11,#]

Affiliations

[1]The Donnelly Centre, University of Toronto, 160 College St., Toronto ON, Canada M5S 3E1

[2]Department of Computer Science & Engineering, University of Minnesota-Twin Cities, 200 Union St., Minneapolis MN, U.S.A. 55455

[3]Simons Center for Data Analysis, Simons Foundation, 160 Fifth Avenue, New York, NY, U.S.A., 10010

[4]Lewis-Sigler Institute for Integrative Genomics, Princeton University, Princeton, NJ, USA, 08544

[5]Department of Molecular Genetics, University of Toronto, 160 College St., Toronto ON, Canada M5S 3E1

[6]Department of Developmental, Molecular and Chemical Biology, Tufts University School of Medicine, Boston, MA, U.S.A. 02111

[7]European Molecular Biology Laboratory (EMBL), Genome Biology Unit, 69117 Heidelberg, Germany

[8]Division of Signaling and Functional Genomics, German Cancer Research Center (DKFZ) and Heidelberg University, Heidelberg, Germany

[9]Lunenfeld-Tanenbaum Research Institute, Mount Sinai Hospital, Toronto ON, Canada

[10]Program in Biomedical Informatics and Computational Biology, University of Minnesota-Twin Cities, 200 Union St., Minneapolis MN, U.S.A. 55455

[11]Chemical Genomics Research Group, RIKEN Center for Sustainable Resource Sciences (CSRS), Saitama, Japan

[12]Princess Margret Cancer Centre, University Health Network & Department of Medical Biophysics, University of Toronto, Toronto ON, Canada

[13]Department of Integrated Biosciences, Graduate School of Frontier Sciences, University of Tokyo, Kashiwa, Chiba, Japan 277-8561

[14]Computer Science Dept., University College London, London, United Kingdom, WC1E 6BT

[15]Department of Computing, Imperial College London, United Kingdom

[16]School of Computing (RAF), Union University, Belgrade

[17]Department of Biochemistry, University of Toronto, Toronto ON, Canada

[18]School of Electronic Information and Communications, Huazhong University of Science and Technology, Wuhan, China, 430074

[19]Department of Genetics, School of Medicine and Stanford Genome Technology Center Stanford University, Palo Alto, CA, U.S.A., 94304

Acknowledgments

We thank David Botstein, Howard Bussey, Andrew Fraser, Helena Friesen, Marc Meneghini, and Michael Tyers for critical comments. This work was primarily supported by the National Institutes of Health (R01HG005853)(C.B., B.A., C.L.M.), Canadian Institutes of Health Research (FDN-143264 and FDN-143265)(C.B., B.A.), RIKEN Strategic Programs for R&D (C.B.), JSPS Kakenhi (15H04483) (C.B.), National Institutes of Health (R01HG005084 and R01GM104975)(C.L.M) and the National Science Foundation (DBI\0953881)(C.L.M.). Computing resources and data storage services were partially provided by the Minnesota Supercomputing Institute and the UMN Office of Information Technology, respectively. Additional support was provided by the Canadian Institutes of Health Research (A.A.C.), National Science Foundation (MCB\1244043) (C.M.), European Research Council Advanced Investigator Grant (AdG-294542) (L.M.S), ERC Advanced Grant (European Commission) (M.B.), Ministry of Education, Culture, Sports, Sciences and Technology, MEXT (15H04402) (Y.O.), Canadian Institutes of Health Research (FDN143301), Genome Canada Genome Innovation network (through the Ontario Genomics Institute)(A.C.G), the Ontario Genomics Institute, Canadian Cystic Fibrosis Foundation, Canadian Cancer Society, Pancreatic Cancer Canada, University Health Network (I.S.), National Science Foundation, Cyber-Enabled Discover and Innovation (CDI) (OIA-1028394), European Research Council (ERC) Starting Independent Researcher Grant (278212), ARRS project (J1-5424), Serbian Ministry of Education and Science Project 11144006 (N.P.), National Natural Science Foundation of China (T.X), RIKEN Foreign Postdoctoral Researcher Program (J.S.P., S.C.L.), National Science Foundation Graduate Research Fellowship (NSF 00039202) (S.W.S). O.G.T, C.L.M, B.A. and C.B are fellows of the Canadian Institute for Advanced Research (CIFAR). All data files associated with this study are available as supplementary materials. Data Files S1–S17 were also deposited in the DRYAD Digital Repository (doi:10.5061/dryad.4291s). Raw mass spectrometry data and downloadable identification and SAINTexpress results tables were deposited in the MassIVE repository housed at the Center for Computational Mass Spectrometry at UCSD (http://proteomics.ucsd.edu/ProteoSAFe/datasets.jsp). The endogenously-tagged GFP and Gal-inducible HA datasets have been assigned the MassIVE IDs MSV000079157 and MSV000079368, and are available for FTP download at: ftp://MSV000079157@massive.ucsd.edu and ftp://

MSV000079368@massive.ucsd.edu, respectively. The datasets were assigned the ProteomeXchange Consortium (http://proteomecentral.proteomexchange.org) identifiers PXD002368 and PXD003147 (dataset password: SGA).

References

1. Costanzo M, et al. The genetic landscape of a cell. Science. 2010; 327:425. [PubMed: 20093466]
2. Hartman, JLt, Garvik, B., Hartwell, L. Principles for the buffering of genetic variation. Science. 2001; 291:1001. [PubMed: 11232561]
3. Zuk O, Hechter E, Sunyaev SR, Lander ES. The mystery of missing heritability: Genetic interactions create phantom heritability. Proc Natl Acad Sci U S A. 2012; 109:1193. [PubMed: 22223662]
4. Bloom JS, et al. Genetic interactions contribute less than additive effects to quantitative trait variation in yeast. Nat Commun. 2015; 6:8712. [PubMed: 26537231]
5. Baryshnikova A, et al. Quantitative analysis of fitness and genetic interactions in yeast on a genome scale. Nat Methods. 2010; 7:1017. [PubMed: 21076421]
6. Roemer T, Boone C. Systems-level antimicrobial drug and drug synergy discovery. Nat Chem Biol. 2013; 9:222. [PubMed: 23508188]
7. Bryant HE, et al. Specific killing of BRCA2-deficient tumours with inhibitors of poly(ADP-ribose) polymerase. Nature. 2005; 434:913. [PubMed: 15829966]
8. Materials and Methods are available as supporting online material.
9. Winzeler EA, et al. Functional characterization of the S. cerevisiae genome by gene deletion and parallel analysis. Science. 1999; 285:901. [PubMed: 10436161]
10. Giaever G, et al. Functional profiling of the Saccharomyces cerevisiae genome. Nature. 2002; 418:387. [PubMed: 12140549]
11. Kofoed M, et al. An Updated Collection of Sequence Barcoded Temperature-Sensitive Alleles of Yeast Essential Genes. G3 (Bethesda). 2015; 5:1879. [PubMed: 26175450]
12. Li Z, et al. Systematic exploration of essential yeast gene function with temperature-sensitive mutants. Nature biotechnology. 2011; 29:361.
13. Schuldiner M, et al. Exploration of the function and organization of the yeast early secretory pathway through an epistatic miniarray profile. Cell. 2005; 123:507. [PubMed: 16269340]
14. Ashburner M, et al. Gene ontology: tool for the unification of biology. The Gene Ontology Consortium. Nat Genet. 2000; 25:25. [PubMed: 10802651]
15. Baryshnikova A. Systematic Functional Annotation and Visualization of Biological Networks. Cell Syst. 2016
16. Dutkowski J, et al. A gene ontology inferred from molecular networks. Nat Biotechnol. 2013; 31:38. [PubMed: 23242164]
17. Koh JL, et al. CYCLoPs: A Comprehensive Database Constructed from Automated Analysis of Protein Abundance and Subcellular Localization Patterns in Saccharomyces cerevisiae. G3 (Bethesda). 2015; 5:1223. [PubMed: 26048563]
18. Sangster TA, Lindquist S, Queitsch C. Under cover: causes, effects and implications of Hsp90-mediated genetic capacitance. BioEssays: news and reviews in molecular, cellular and developmental biology. 2004; 26:348.
19. Chan S, Choi EA, Shi Y. Pre-mRNA 3′-end processing complex assembly and function. Wiley interdisciplinary reviews RNA. 2011; 2:321. [PubMed: 21957020]
20. Gordon JM, et al. Reconstitution of CF IA from overexpressed subunits reveals stoichiometry and provides insights into molecular topology. Biochemistry. 2011; 50:10203. [PubMed: 22026644]
21. Abe F, Minegishi H. Global screening of genes essential for growth in high-pressure and cold environments: searching for basic adaptive strategies using a yeast deletion library. Genetics. 2008; 178:851. [PubMed: 18245339]
22. Addinall SG, et al. A genomewide suppressor and enhancer analysis of cdc13-1 reveals varied cellular processes influencing telomere capping in Saccharomyces cerevisiae. Genetics. 2008; 180:2251. [PubMed: 18845848]

23. Greenall A, et al. A genome wide analysis of the response to uncapped telomeres in budding yeast reveals a novel role for the NAD+ biosynthetic gene BNA2 in chromosome end protection. Genome Biol. 2008; 9:R146. [PubMed: 18828915]
24. Mnaimneh S, et al. Exploration of essential gene functions via titratable promoter alleles. Cell. 2004; 118:31. [PubMed: 15242642]
25. Koch EN, et al. Conserved rules govern genetic interaction degree across species. Genome biology. 2012; 13:R57. [PubMed: 22747640]
26. Lahiri S, et al. A conserved endoplasmic reticulum membrane protein complex (EMC) facilitates phospholipid transfer from the ER to mitochondria. PLoS Biol. 2014; 12:e1001969. [PubMed: 25313861]
27. Sanchez R, Sali A. Large-scale protein structure modeling of the Saccharomyces cerevisiae genome. Proc Natl Acad Sci U S A. 1998; 95:13597. [PubMed: 9811845]
28. Segre D, Deluna A, Church GM, Kishony R. Modular epistasis in yeast metabolism. Nat Genet. 2005; 37:77. [PubMed: 15592468]
29. Bandyopadhyay S, Kelley R, Krogan NJ, Ideker T. Functional maps of protein complexes from quantitative genetic interaction data. PLoS Comput Biol. 2008; 4:e1000065. [PubMed: 18421374]
30. Hoepfner D, et al. High-resolution chemical dissection of a model eukaryote reveals targets, pathways and gene functions. Microbiol Res. 2014; 169:107. [PubMed: 24360837]
31. Bell SP. The origin recognition complex: from simple origins to complex functions. Genes Dev. 2002; 16:659. [PubMed: 11914271]
32. Lei M, Tye BK. Initiating DNA synthesis: from recruiting to activating the MCM complex. J Cell Sci. 2001; 114:1447. [PubMed: 11282021]
33. MacNeill SA. Structure and function of the GINS complex, a key component of the eukaryotic replisome. Biochem J. 2010; 425:489. [PubMed: 20070258]
34. Peters JM. The anaphase promoting complex/cyclosome: a machine designed to destroy. Nat Rev Mol Cell Biol. 2006; 7:644. [PubMed: 16896351]
35. Khosrow-Khavar F, et al. The yeast ubr1 ubiquitin ligase participates in a prominent pathway that targets cytosolic thermosensitive mutants for degradation. G3 (Bethesda). 2012; 2:619. [PubMed: 22670231]
36. Li R, Murray AW. Feedback control of mitosis in budding yeast. Cell. 1991; 66:519. [PubMed: 1651172]
37. Bandyopadhyay S, et al. Rewiring of genetic networks in response to DNA damage. Science. 2010; 330:1385. [PubMed: 21127252]
38. Hutchison CA 3rd, et al. Design and synthesis of a minimal bacterial genome. Science. 2016; 351:aad6253. [PubMed: 27013737]
39. Dowell RD, et al. Genotype to phenotype: a complex problem. Science. 2010; 328:469. [PubMed: 20413493]
40. VanderSluis B, et al. Genetic interactions reveal the evolutionary trajectories of duplicate genes. Molecular Systems Biology. 2010; 6:429. [PubMed: 21081923]
41. Altshuler D, Daly MJ, Lander ES. Genetic mapping in human disease. Science. 2008; 322:881. [PubMed: 18988837]
42. Lehner B, Crombie C, Tischler J, Fortunato A, Fraser AG. Systematic mapping of genetic interactions in Caenorhabditis elegans identifies common modifiers of diverse signaling pathways. Nat Genet. 2006; 38:896. [PubMed: 16845399]
43. Byrne AB, et al. A global analysis of genetic interactions in Caenorhabditis elegans. J Biol. 2007; 6:8. [PubMed: 17897480]
44. Fischer B, et al. A map of directional genetic interactions in a metazoan cell. Elife. 2015; 4
45. Blekhman R, et al. Host genetic variation impacts microbiome composition across human body sites. Genome Biol. 2015; 16:191. [PubMed: 26374288]
46. Buchovecky CM, et al. A suppressor screen in Mecp2 mutant mice implicates cholesterol metabolism in Rett syndrome. Nature genetics. 2013; 45:1013. [PubMed: 23892605]
47. Keeling KM, Xue X, Gunn G, Bedwell DM. Therapeutics based on stop codon readthrough. Annu Rev Genomics Hum Genet. 2014; 15:371. [PubMed: 24773318]

48. Tsvetkov P, et al. Compromising the 19S proteasome complex protects cells from reduced flux through the proteasome. Elife. 2015; 4
49. Dixon SJ, et al. Significant conservation of synthetic lethal genetic interaction networks between distantly related eukaryotes. Proc Natl Acad Sci U S A. 2008; 105:16653. [PubMed: 18931302]
50. Roguev A, et al. Conservation and rewiring of functional modules revealed by an epistasis map in fission yeast. Science. 2008; 322:405. [PubMed: 18818364]
51. Deshpande R, et al. A comparative genomic approach for identifying synthetic lethal interactions in human cancer. Cancer research. 2013; 73:6128. [PubMed: 23980094]
52. McManus KJ, Barrett IJ, Nouhi Y, Hieter P. Specific synthetic lethal killing of RAD54B-deficient human colorectal cancer cells by FEN1 silencing. Proc Natl Acad Sci U S A. 2009; 106:3276. [PubMed: 19218431]
53. van Pel DM, et al. An evolutionarily conserved synthetic lethal interaction network identifies FEN1 as a broad-spectrum target for anticancer therapeutic development. PLoS Genet. 2013; 9:e1003254. [PubMed: 23382697]
54. Hartwell LH, Szankasi P, Roberts CJ, Murray AW, Friend SH. Integrating genetic approaches into the discovery of anticancer drugs. Science. 1997; 278:1064. [PubMed: 9353181]
55. Hart T, et al. High-Resolution CRISPR Screens Reveal Fitness Genes and Genotype-Specific Cancer Liabilities. Cell. 2015; 163:1515. [PubMed: 26627737]
56. Wang T, et al. Identification and characterization of essential genes in the human genome. Science. 2015; 350:1096. [PubMed: 26472758]
57. Blomen VA, et al. Gene essentiality and synthetic lethality in haploid human cells. Science. 2015; 350:1092. [PubMed: 26472760]
58. Ben-Aroya S, et al. Toward a comprehensive temperature-sensitive mutant repository of the essential genes of Saccharomyces cerevisiae. Mol Cell. 2008; 30:248. [PubMed: 18439903]
59. Kuzmin E, et al. Synthetic genetic array analysis for global mapping of genetic networks in yeast. Methods Mol Biol. 2014; 1205:143. [PubMed: 25213244]
60. Deshpande R, Vandersluis B, Myers CL. Comparison of profile similarity measures for genetic interaction networks. PLoS One. 2013; 8:e68664. [PubMed: 23874711]
61. Shannon P, et al. Cytoscape: a software environment for integrated models of biomolecular interaction networks. Genome Res. 2003; 13:2498. [PubMed: 14597658]
62. Myers CL, Barrett DR, Hibbs MA, Huttenhower C, Troyanskaya OG. Finding function: evaluation methods for functional genomic data. BMC Genomics. 2006; 7:187. [PubMed: 16869964]
63. Bellay J, et al. Putting genetic interactions in context through a global modular decomposition. Genome Research. 2011; 21:1375. [PubMed: 21715556]
64. Zhao R, et al. Navigating the chaperone network: an integrative map of physical and genetic interactions mediated by the hsp90 chaperone. Cell. 2005; 120:715. [PubMed: 15766533]
65. Subramanian A, et al. Gene set enrichment analysis: a knowledge-based approach for interpreting genome-wide expression profiles. Proc Natl Acad Sci U S A. 2005; 102:15545. [PubMed: 16199517]
66. Zhao J, Kessler M, Helmling S, O'Connor JP, Moore C. Pta1, a component of yeast CF II, is required for both cleavage and poly(A) addition of mRNA precursor. Mol Cell Biol. 1999; 19:7733. [PubMed: 10523662]
67. Wilkening S, et al. An efficient method for genome-wide polyadenylation site mapping and RNA quantification. Nucleic Acids Res. 2013; 41:e65. [PubMed: 23295673]
68. Wu TD, Nacu S. Fast and SNP-tolerant detection of complex variants and splicing in short reads. Bioinformatics. 2010; 26:873. [PubMed: 20147302]
69. Xu Z, et al. Bidirectional promoters generate pervasive transcription in yeast. Nature. 2009; 457:1033. [PubMed: 19169243]
70. Love MI, Huber W, Anders S. Moderated estimation of fold change and dispersion for RNA-seq data with DESeq2. Genome Biol. 2014; 15:550. [PubMed: 25516281]
71. Huh WK, et al. Global analysis of protein localization in budding yeast. Nature. 2003; 425:686. [PubMed: 14562095]

72. Taipale M, et al. A quantitative chaperone interaction network reveals the architecture of cellular protein homeostasis pathways. Cell. 2014; 158:434. [PubMed: 25036637]
73. Kessner D, Chambers M, Burke R, Agus D, Mallick P. ProteoWizard: open source software for rapid proteomics tools development. Bioinformatics. 2008; 24:2534. [PubMed: 18606607]
74. Perkins DN, Pappin DJ, Creasy DM, Cottrell JS. Probability-based protein identification by searching sequence databases using mass spectrometry data. Electrophoresis. 1999; 20:3551. [PubMed: 10612281]
75. Eng JK, Jahan TA, Hoopmann MR. Comet: an open-source MS/MS sequence database search tool. Proteomics. 2013; 13:22. [PubMed: 23148064]
76. Shteynberg D, et al. iProphet: multi-level integrative analysis of shotgun proteomic data improves peptide and protein identification rates and error estimates. Mol Cell Proteomics. 2011; 10:M111 007690.
77. Teo G, et al. SAINTexpress: improvements and additional features in Significance Analysis of INTeractome software. J Proteomics. 2014; 100:37. [PubMed: 24513533]
78. Mellacheruvu D, et al. The CRAPome: a contaminant repository for affinity purification-mass spectrometry data. Nat Methods. 2013; 10:730. [PubMed: 23921808]
79. Gelperin DM, et al. Biochemical and genetic analysis of the yeast proteome with a movable ORF collection. Genes and Development. 2005; 19:2816. [PubMed: 16322557]
80. Srikumar T, Lewicki MC, Raught B. A global S. cerevisiae small ubiquitin-related modifier (SUMO) system interactome. Mol Syst Biol. 2013; 9:668. [PubMed: 23712011]
81. Craig R, Beavis RC. TANDEM: matching proteins with tandem mass spectra. Bioinformatics. 2004; 20:1466. [PubMed: 14976030]
82. Vida TA, Emr SD. A new vital stain for visualizing vacuolar membrane dynamics and endocytosis in yeast. J Cell Biol. 1995; 128:779. [PubMed: 7533169]
83. Saenz DA, Chianelli MS, Stella CA. L-Phenylalanine Transport in Saccharomyces cerevisiae: Participation of GAP1, BAP2, and AGP1. J Amino Acids. 2014; 2014:283962. [PubMed: 24701347]
84. Gibney PA, Lu C, Caudy AA, Hess DC, Botstein D. Yeast metabolic and signaling genes are required for heat-shock survival and have little overlap with the heat-induced genes. Proc Natl Acad Sci U S A. 2013; 110:E4393. [PubMed: 24167267]
85. Rosebrock, AP., Caudy, AA. Metabolomic Analysis of Budding Yeast. In: Andrews, B.Boone, C.Davis, T., Fields, S., editors. Budding Yeast: A Laboratory Manual. Cold Spring Harbor Press; 2016. p. 599-620.
86. Wan LC, et al. Reconstitution and characterization of eukaryotic N6-threonylcarbamoylation of tRNA using a minimal enzyme system. Nucleic Acids Res. 2013; 41:6332. [PubMed: 23620299]
87. Ostlund G, et al. InParanoid 7: new algorithms and tools for eukaryotic orthology analysis. Nucleic Acids Res. 2010; 38:D196. [PubMed: 19892828]
88. Wapinski I, Pfeffer A, Friedman N, Regev A. Natural history and evolutionary principles of gene duplication in fungi. Nature. 2007; 449:54. [PubMed: 17805289]
89. Rice P, Longden I, Bleasby A. EMBOSS: the European Molecular Biology Open Software Suite. Trends Genet. 2000; 16:276. [PubMed: 10827456]
90. Hillenmeyer ME, et al. The chemical genomic portrait of yeast: uncovering a phenotype for all genes. Science. 2008; 320:362. [PubMed: 18420932]
91. Huttenhower C, Hibbs M, Myers C, Troyanskaya OG. A scalable method for integration and functional analysis of multiple microarray datasets. Bioinformatics. 2006; 22:2890. [PubMed: 17005538]
92. Liti G, et al. Population genomics of domestic and wild yeasts. Nature. 2009; 458:337. [PubMed: 19212322]
93. Jelier R, Semple JI, Garcia-Verdugo R, Lehner B. Predicting phenotypic variation in yeast from individual genome sequences. Nat Genet. 2011; 43:1270. [PubMed: 22081227]
94. Yang Z. PAML 4: phylogenetic analysis by maximum likelihood. Mol Biol Evol. 2007; 24:1586. [PubMed: 17483113]

95. Edgar RC. MUSCLE: a multiple sequence alignment method with reduced time and space complexity. BMC Bioinformatics. 2004; 5:113. [PubMed: 15318951]

96. Holstege F, et al. Dissecting the Regulatory Circuitry of a Eukaryotic Genome. Cell. 1998; 95:717. [PubMed: 9845373]

97. Gasch AP, et al. Genomic expression programs in the response of yeast cells to environmental changes. Mol Biol Cell. 2000; 11:4241. [PubMed: 11102521]

98. Brem RB, Storey JD, Whittle J, Kruglyak L. Genetic interactions between polymorphisms that affect gene expression in yeast. Nature. 2005; 436:701. [PubMed: 16079846]

99. Skelly DA, et al. Integrative phenomics reveals insight into the structure of phenotypic diversity in budding yeast. Genome Res. 2013; 23:1496. [PubMed: 23720455]

100. Byrne KP, Wolfe KH. The Yeast Gene Order Browser: combining curated homology and syntenic context reveals gene fate in polyploid species. Genome Research. 2005; 15:1456. [PubMed: 16169922]

101. Gu Z, Cavalcanti A, Chen FC, Bouman P, Li WH. Extent of gene duplication in the genomes of Drosophila, nematode, and yeast. Mol Biol Evol. 2002; 19:256. [PubMed: 11861885]

102. Rost B. Twilight zone of protein sequence alignments. Protein Eng. 1999; 12:85. [PubMed: 10195279]

103. Levy SF, Siegal ML. Network hubs buffer environmental variation in Saccharomyces cerevisiae. PLoS Biol. 2008; 6:e264. [PubMed: 18986213]

104. Gavin AC, et al. Proteome survey reveals modularity of the yeast cell machinery. Nature. 2006; 440:631. [PubMed: 16429126]

105. Krogan NJ, et al. Global landscape of protein complexes in the yeast Saccharomyces cerevisiae. Nature. 2006; 440:637. [PubMed: 16554755]

106. Yu H, et al. High-quality binary protein interaction map of the yeast interactome network. Science. 2008; 322:104. [PubMed: 18719252]

107. Newman JR, et al. Single-cell proteomic analysis of S. cerevisiae reveals the architecture of biological noise. Nature. 2006; 441:840. [PubMed: 16699522]

108. Ward JJ, McGuffin LJ, Bryson K, Buxton BF, Jones DT. The DISOPRED server for the prediction of protein disorder. Bioinformatics. 2004; 20:2138. [PubMed: 15044227]

109. Stark C, et al. The BioGRID Interaction Database: 2011 update. Nucleic Acids Res. 2011; 39:D698. [PubMed: 21071413]

110. Tarassov K, et al. An in vivo map of the yeast protein interactome. Science. 2008; 320:1465. [PubMed: 18467557]

111. Babu M, et al. Interaction landscape of membrane-protein complexes in Saccharomyces cerevisiae. Nature. 2012; 489:585. [PubMed: 22940862]

112. Piotrowski JS, et al. Plant-derived antifungal agent poacic acid targets beta-1,3-glucan. Proc Natl Acad Sci U S A. 2015; 112:E1490. [PubMed: 25775513]

113. Kato N, Takahashi S, Nogawa T, Saito T, Osada H. Construction of a microbial natural product library for chemical biology studies. Curr Opin Chem Biol. 2012; 16:101. [PubMed: 22406171]

114. Piotrowski JS, et al. Chemical genomic profiling via barcode sequencing to predict compound mode of action. Methods Mol Biol. 2015; 1263:299. [PubMed: 25618354]

115. Fung SY, et al. Unbiased screening of marine sponge extracts for anti-inflammatory agents combined with chemical genomics identifies girolline as an inhibitor of protein synthesis. ACS Chem Biol. 2014; 9:247. [PubMed: 24117378]

116. Bukhman Y, et al. Modeling Microbial growth with GCAT. Bioenergy Research. 2015; 8:1022–1030.

117. Benschop JJ, et al. A consensus of core protein complex compositions for Saccharomyces cerevisiae. Mol Cell. 2010; 38:916. [PubMed: 20620961]

118. Finley D, Ulrich HD, Sommer T, Kaiser P. The ubiquitin-proteasome system of Saccharomyces cerevisiae. Genetics. 2012; 192:319. [PubMed: 23028185]

119. Chong YT, et al. Yeast Proteome Dynamics from Single Cell Imaging and Automated Analysis. Cell. 2015; 161:1413. [PubMed: 26046442]

120. Kanehisa M, et al. Data, information, knowledge and principle: back to metabolism in KEGG. Nucleic Acids Res. 2014; 42:D199. [PubMed: 24214961]

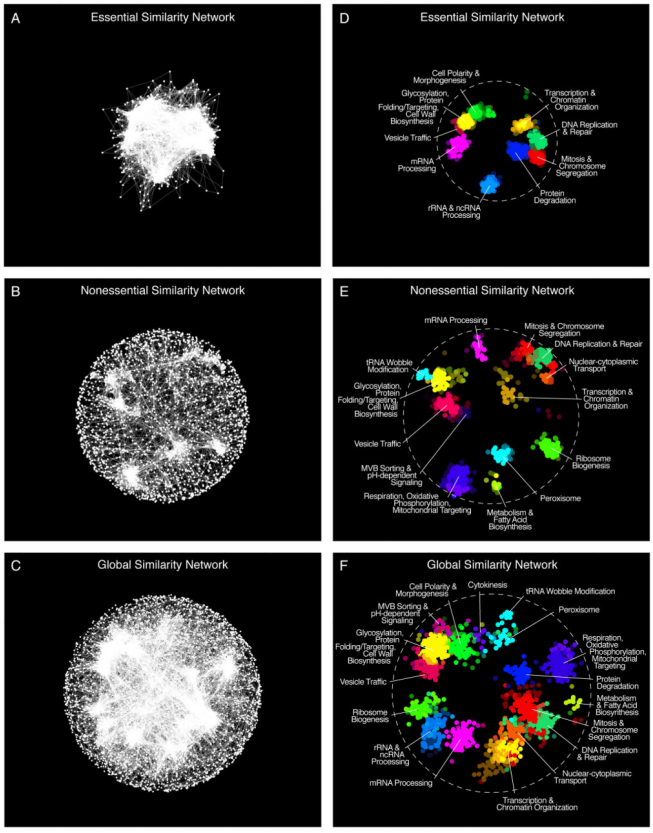

Figure 1. A global network of genetic interaction profile similarities

(A) The essential similarity network was constructed by computing Pearson correlation coefficients (PCCs) for genetic interaction profiles (edges) of all pairs of genes (nodes) in the essential genetic interaction matrix (ExE). Gene pairs whose profile similarity exceeded a PCC > 0.2 were connected and graphed using a spring-embedded layout algorithm. Genes sharing similar genetic interactions profiles map proximal to each other, whereas genes with less similar genetic interaction profiles are positioned further apart. (**B**) A genetic profile similarity network for the nonessential genetic interaction matrix (NxN). (**C**) A global genetic profile similarity network encompassing all nonessential and essential genes was constructed from the combined NxN, ExE and NxE genetic interaction matrices. **(D)** The essential similarity network was annotated using the Spatial Analysis of Functional Enrichment (SAFE), identifying network regions enriched for similar GO biological process terms, which are color-coded. (**E**) The nonessential similarity network annotated using SAFE. (**F**) The global similarity network annotated using SAFE.

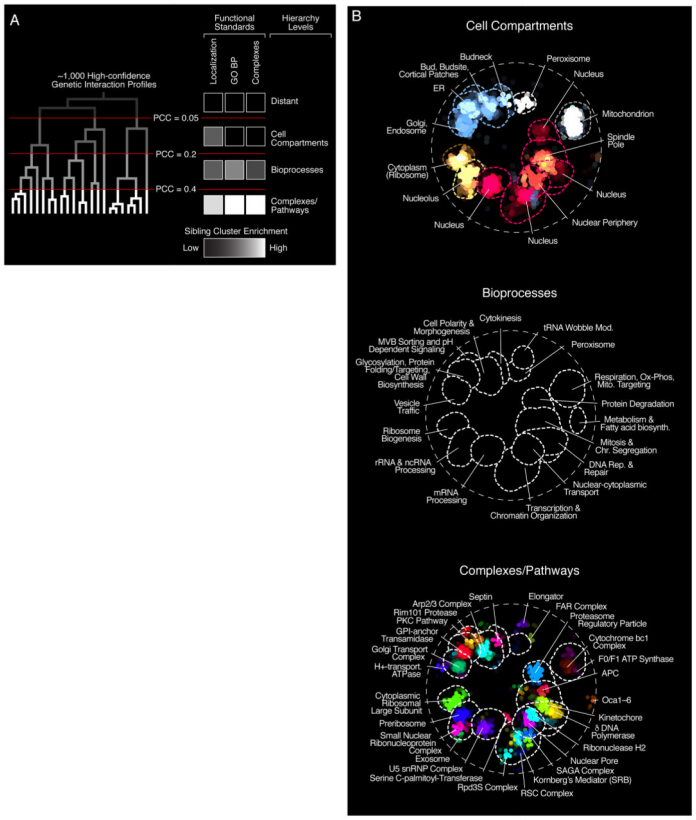

Figure 2. The global genetic interaction profile similarity network reveals a hierarchy of cellular function

(A) A schematic representation of a genetic interaction profile-derived hierarchy. Genes with highly correlated genetic interaction profiles (PCC > 0.4) form small, densely connected clusters representing specific pathways or protein complexes. At an intermediate range of profile similarity (0.2 < PCC < 0.4), sibling clusters representing distinct pathway or complexes combine together into larger biological process enriched clusters. At a lower range of profile similarity (0.05 < PCC < 0.2), bioprocess-enriched clusters, in turn, combine together to form larger clusters corresponding to different cell compartments. The grey-white scale bar illustrates enrichment of sibling clusters for the same set of terms from the indicated functional standard. See also fig. S7. (**B**) The genetic network hierarchy visualized using SAFE analysis, which identified regions in the global similarity network enriched for specific cellular compartments, biological processes or protein complexes.

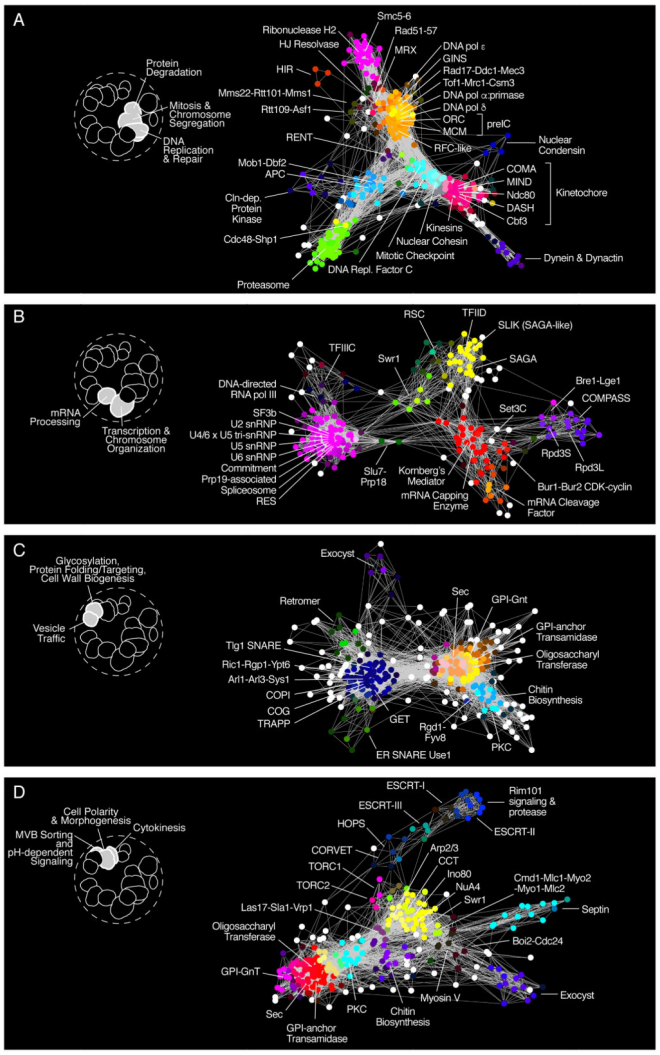

Figure 3. Genetic interaction profile similarity sub-networks

Genes belonging to the indicated biological process-enriched clusters were extracted from the global network and laid out using a spring-embedded layout algorithm. Sub-networks were annotated using SAFE to identify network regions enriched for specific protein complexes. **(A)** Protein complexes localized within the Protein Degradation, Mitosis & Chromosome Segregation, and DNA Replication & Repair, enriched bioprocess clusters shown in Fig. 1F. **(B)** Protein complexes localized within the Transcription & Chromatin Organization and mRNA Processing-enriched bioprocess clusters shown in Fig. 1F. **(C)** Protein complexes localized within the Glycosylation, Protein folding/Targeting, Cell Wall Biosynthesis and Vesicle Traffic-enriched bioprocess clusters shown in Fig. 1F. **(D)** Protein complexes localized within the MVB Sorting & pH-dependent Signaling, Cell Polarity & Morphogenesis, and Cytokinesis enriched bioprocess clusters shown in Fig. 1F.

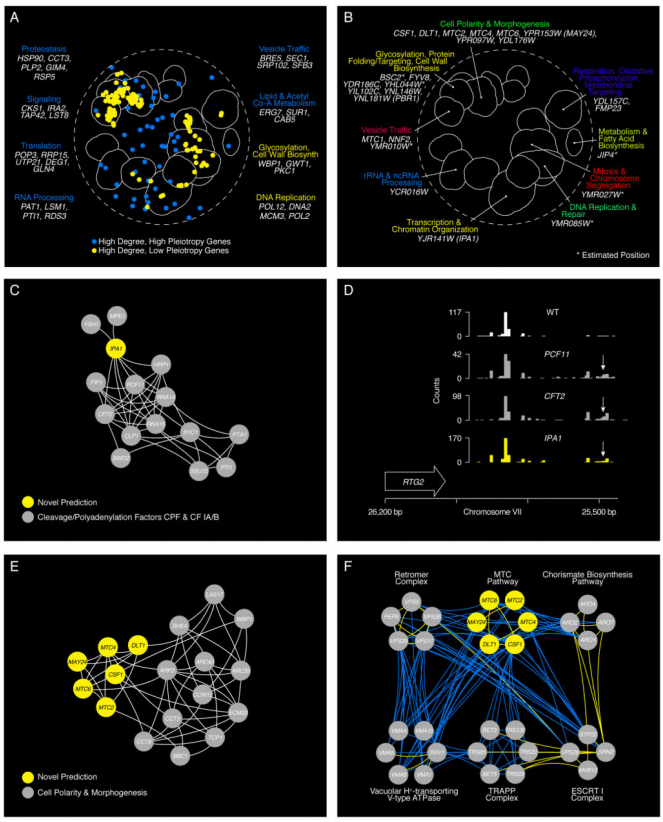

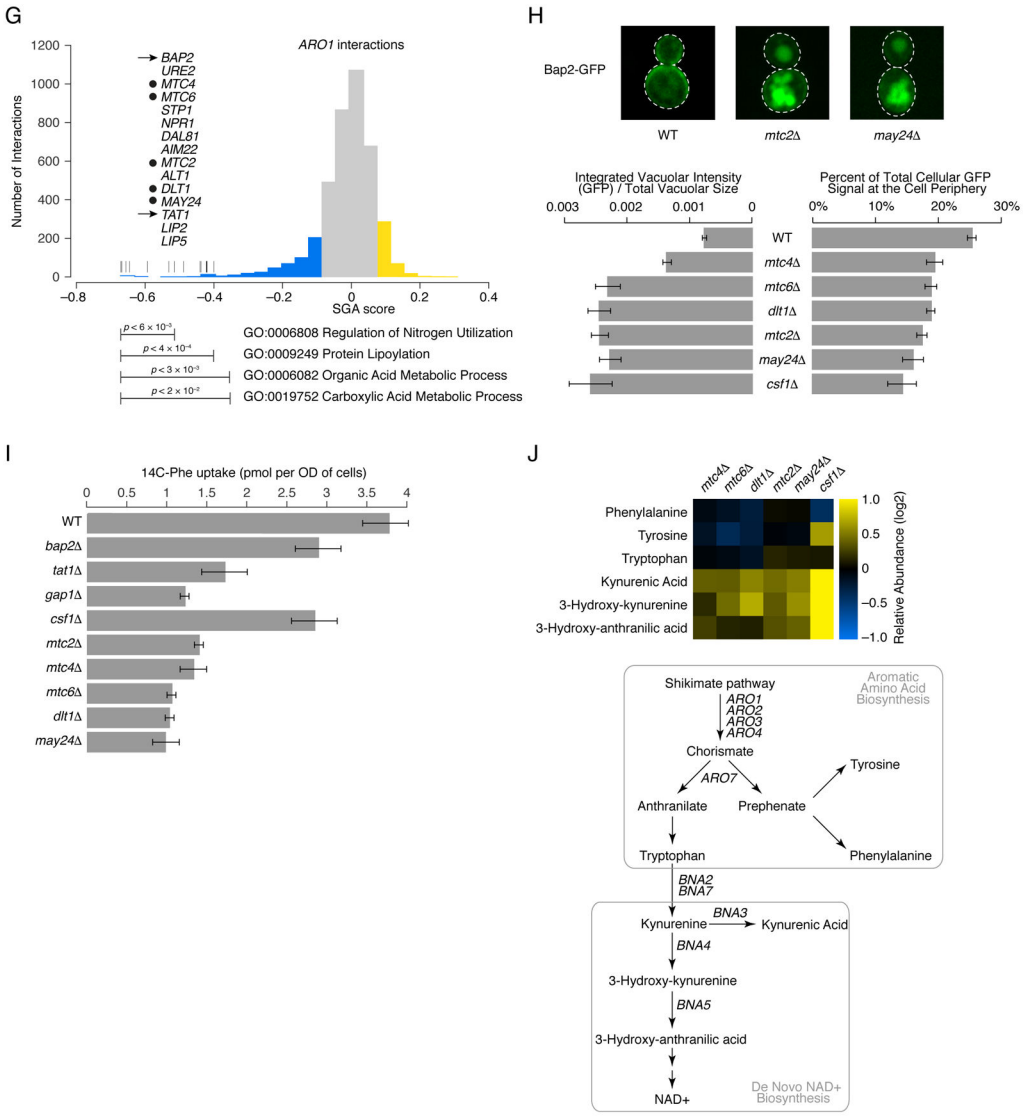

Figure 4. Using network connectivity to explore gene function

(A) Highly connected hub genes identified either as pleiotropic (blue nodes), or functionally specific (yellow nodes), are highlighted on a schematic representation of the global similarity network. Examples of high (blue text) and low (yellow text) pleiotropy genes, grouped based on their general function, are shown. **(B)** Poorly characterized genes that localize within, or in the vicinity of, a specific biological process-enriched cluster on the global similarity network. For genes whose genetic interaction profile similarity to other genes does not exceed a PCC > 0.2 and would otherwise not appear on the global similarity network, an estimated position based on the most similar genes appearing in the network is indicated (*). **(C)** A genetic interaction profile similarity subnetwork for the uncharacterized essential gene, *IPA1* (yellow node), extracted from the Transcription & Chromatin Organization enriched biological process cluster. **(D)** Polyadenylation profiles for a representative gene, *RTG2*, generated from genome-wide sequencing of mRNA purified from a wild-type strain (WT) and strains carrying TS mutations of *PCF11*, *CFT2* or *IPA1.*

The horizontal arrow indicates the orientation of the *RTG2* open reading frame, the vertical arrows indicate the mutant, increased aberrant, 3′ mRNA cleavage and polyadenylation. **(E)** A genetic interaction profile similarity sub-network for *MTC2, MTC4, MTC6, CSF1, DLT1* and *MAY24* genes (yellow nodes) extracted from the network region in the vicinity of the Cell Polarity & Morphogenesis biological process cluster. **(F)** The MTC pathway genetic interaction network. Nodes are grouped according to genetic interaction profile similarity and edges represent negative (blue) and positive (yellow) interactions (genetic interaction score, $|\varepsilon| > 0.08$, $P < 0.05$). **(G)** Distribution of *ARO1* negative (blue) and positive (yellow) genetic interactions ($|\varepsilon| > 0.08$, $P < 0.05$; gene pairs that failed to meet threshold for interactions are colored grey). Functions enriched among genes that displayed an extreme negative interaction with *ARO1* are indicated and a subset of these genes is shown. Closed circles indicate members of the MTC pathway and arrows indicate amino acid permease encoding genes. **(H)** Representative cell images illustrating Bap2-GFP localization in wild type, *mtc2*Δ and *may24*Δ deletion mutant strains (Top panel). Vacuolar intensity (total GFP signal in the vacuole/vacuolar area) and percent of total cellular GFP present at the cell periphery (cell periphery GFP/total cellular GFP signal) were quantified for wild type cells and MTC pathway mutants (Bottom panel). Error bars indicate standard deviation from three replicate experiments. **(I)** Cellular uptake of ^{14}C-labeled phenylalanine in wild type and deletion mutant strains. Error bars indicate standard deviation from three replicate experiments. **(J)** Metabolite levels for the indicated mutants were analyzed by full scan LC-MS (Top panel). The levels of selected metabolites are presented as $\log_2$ ratios relative to wild type cells. Schematic diagram illustrating aromatic amino acid and *de novo* NAD+ biosynthesis pathways (bottom panel).

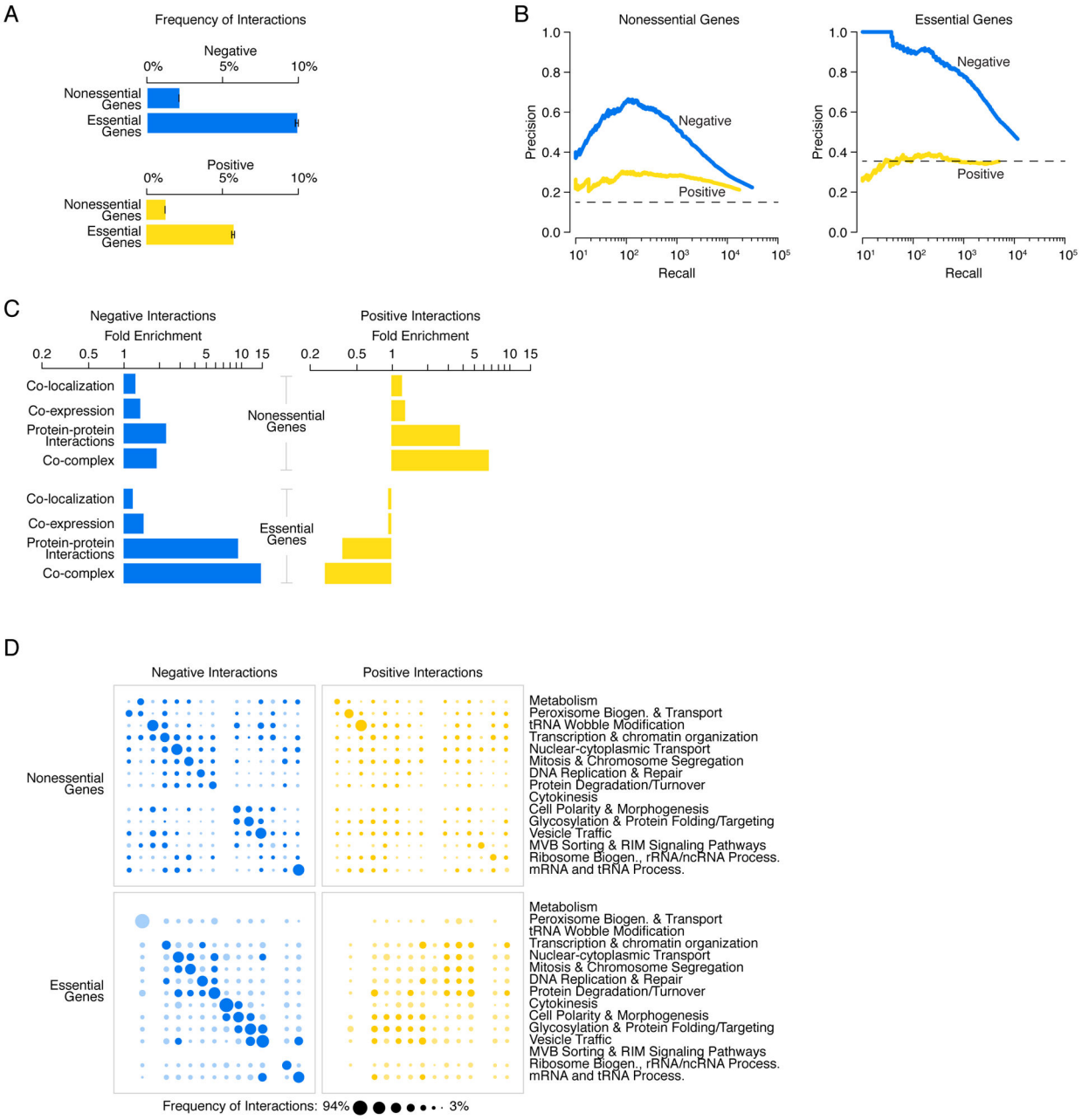

Figure 5. Negative and positive genetic interactions connecting nonessential and essential genes

(A) The network density of negative (blue) and positive (yellow) genetic interactions, expressed as a fraction of all tested gene pairs, associated with nonessential and essential genes, at a defined threshold (genetic interaction score, $|\varepsilon| > 0.08$, $P < 0.05$). Error bars indicate the standard deviation across multiple samplings of the alleles for essential genes, where each gene is represented by a single, randomly selected allele in each sampling. **(B)** Plots of precision versus recall (number of true positives (TP)) for negative (blue) and positive (yellow) interactions for nonessential and essential genes, as determined by our genetic interaction score ($|\varepsilon| > 0.08$, $P < 0.05$). True positive interactions were defined as those involving gene pairs co-annotated to a gold standard set of GO terms. The precision

and recall values were calculated as described (8). **(C)** Fold enrichment for negative (blue) and positive (yellow) genetic interactions among co-localized, co-expressed, or physically interacting, gene pairs were calculated for either nonessential or essential gene pairs. **(D)** Network density of genetic interactions within and across biological processes. The fraction of screened nonessential and essential gene pairs exhibiting negative or positive interactions, as determined by our genetic interaction score ($|\varepsilon| > 0.08$, $P < 0.05$), was measured for the 17 gene sets enriched for specific biological processes, as defined in Fig. 1F. Node size reflects the fraction of interacting gene pairs observed for a given pair of biological processes. Dark blue and dark yellow nodes indicate that the frequency of interaction is significantly above random expectation. Light blue and light yellow nodes represent a frequency of interaction that is not significantly higher than random expectation. Nodes on the diagonal represent the frequency of interactions among genes belonging to the same biological process. Nodes off the diagonal represent the frequency of interactions between different biological processes.

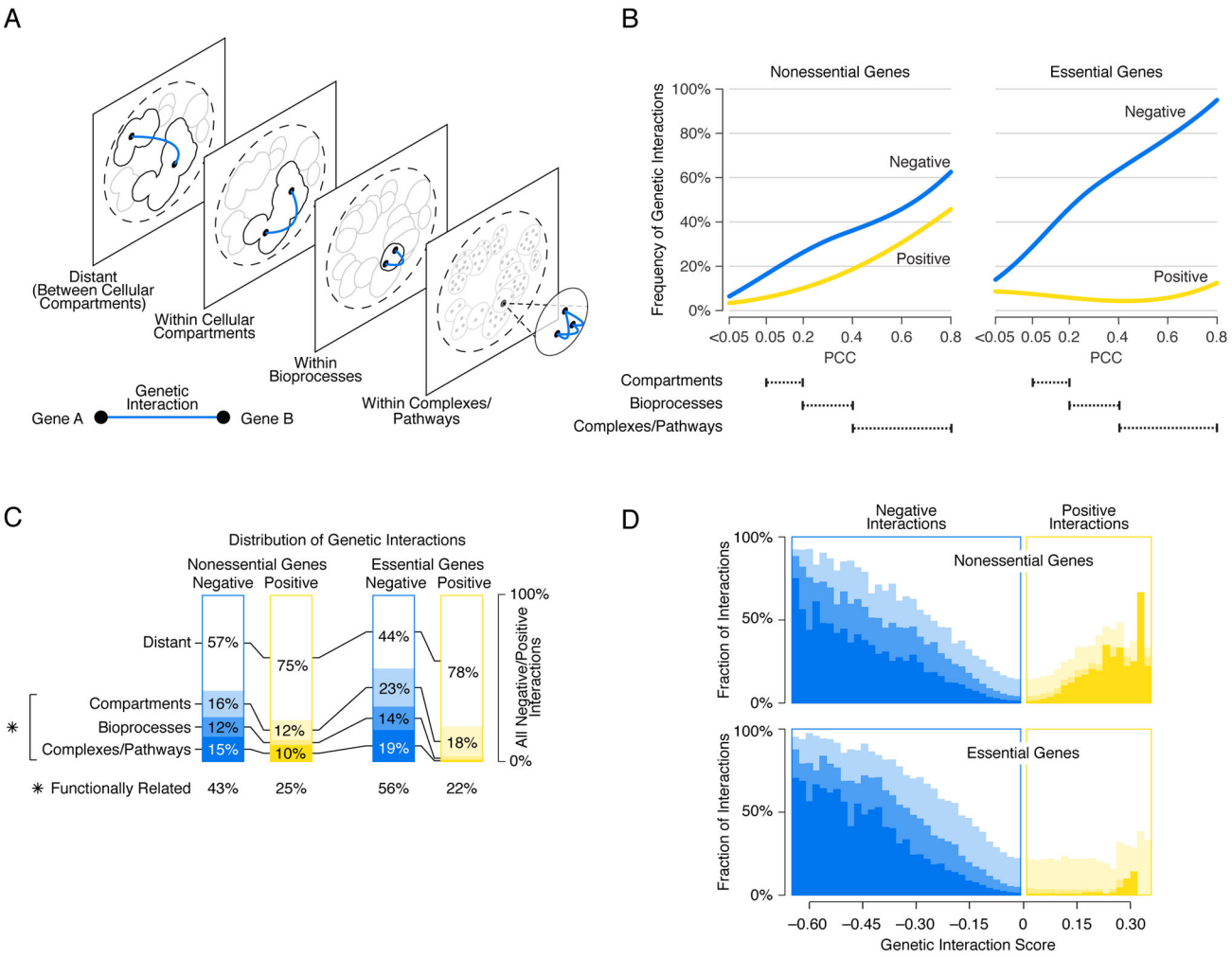

Figure 6. Mapping negative and positive interactions across the genetic network based functional hierarchy

(A) Schematic representation of the genetic network-based functional hierarchy illustrating interactions between genes within the same complex, biological process, or cellular compartment, as well as distant interactions that span different cellular compartments. **(B)** The network density of genetic interactions between genes in the same cluster, at a given level of profile similarity (PCC) in the genetic network hierarchy for negative (blue) or positive (yellow) genetic interactions (genetic interaction score, $|\varepsilon| > 0.08$, $P < 0.05$). Dashed lines indicate the PCC range within which clusters in the genetic network hierarchy were enriched for cell compartments, bioprocesses, and protein complexes. **(C)** The functional distribution of all negative (blue) and all positive (yellow) interactions ($|\varepsilon| > 0.08$, $P < 0.05$) among genes in the genetic network hierarchy. The percentage of all interactions connecting nonessential gene pairs and essential gene pairs in the same clusters corresponding to a cell compartment, bioprocess or complex/pathway is shown. The combined fraction of functionally related interactions (i.e. interactions connecting genes in the same compartment, bioprocess, complex or pathway) is also indicated (*). **(D)** The percentage of negative (blue) and positive (yellow) interactions within a specified genetic interaction score (ε) range that

connects genes belonging to the same cluster at the indicated level of the genetic network-based hierarchy. Different shades of blue and yellow correspond to levels of functional relatedness shown in (C). The white area corresponds to the fraction of interactions that connect genes in different cellular compartments (i.e. Distant).

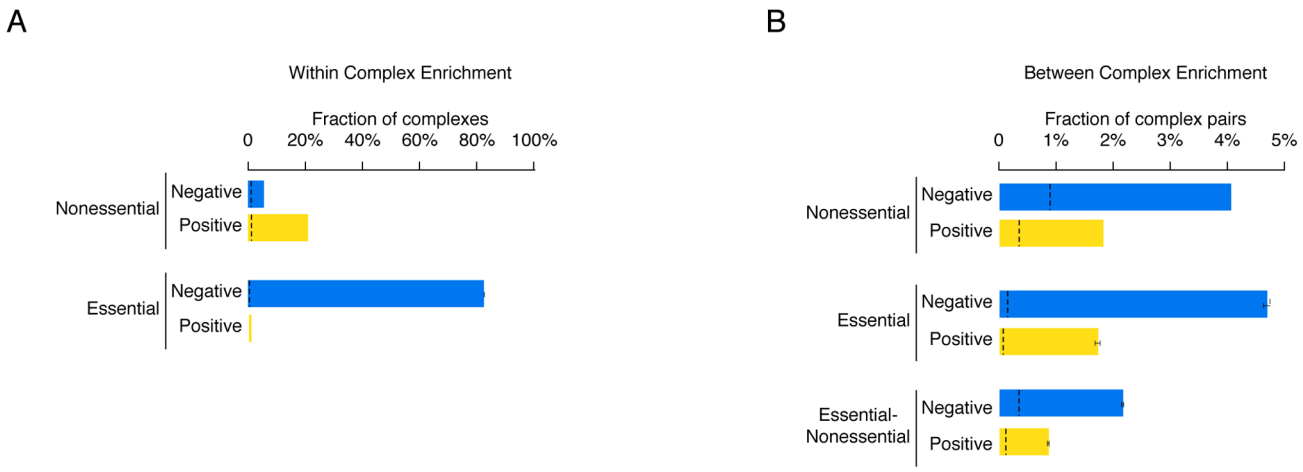

Figure 7. Genetic interactions within and between protein complexes

(A) The percentage of nonessential and essential complexes whose members were enriched for genetic interactions with each other and biased (i.e. coherent) for either mostly negative (blue) or mostly positive (yellow) interactions. **(B)** The percentage of nonessential-nonessential, essential-essential or essential-nonessential complex-complex pairs found to be enriched for genetic interactions and biased (i.e. coherent) for either mostly negative (blue) or mostly positive (yellow) interactions. Black dashed lines indicate the background rate of coherent genetic interaction enrichment within individual complexes or between pairs of protein complexes. Error bars indicate the standard deviation across multiple samplings of the alleles for essential genes, where each gene is represented by a single, randomly selected allele in each sampling.

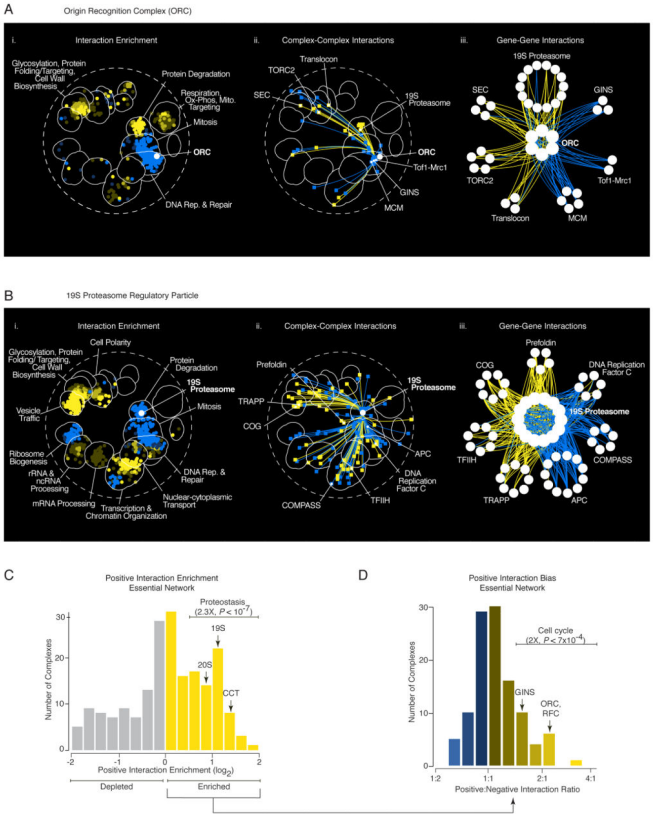

Figure 8. Functional wiring diagrams for specific protein complexes

(A) Genetic interaction map for the ORC (Origin Recognition Complex) (i) Regions of the global similarity network significantly enriched for genes exhibiting negative (blue) or positive (yellow) genetic interactions with ORC members were mapped using SAFE. (ii) Protein complexes that showed coherent negative or positive genetic interactions with ORC were placed on a schematic representation of the global similarity network based on the average genetic interaction profile similarity of the complex and connected with blue or yellow edges, respectively. (iii) A subset of protein complexes from (ii) that showed coherent negative (blue) or positive (yellow) genetic interactions with genes encoding the ORC are shown. **(B)** Genetic interaction map for the 19S proteasome. The 19S proteasome networks shown in (i–iii) were constructed are as described in (A). **(C)** Distribution of positive genetic interaction enrichment for protein complexes screened against the essential gene array (TSA). Protein complexes enriched for positive interactions with essential genes (yellow bars) tend to be associated with proteostasis-related functions (2.3X, $P < 10^{-7}$, Fisher's Exact Test), including the 19S and 20S proteasome subunits as well as the chaperonin-containing T-complex (CCT) and prefoldin chaperone complexes (indicated on the graph). **(D)** Distribution of positive vs. negative genetic interactions for protein complexes enriched for positive interactions shown in (C). Essential protein complexes that show a bias towards positive interactions, such as the ORC, RFC, and GINS, are often required for normal cell cycle progression (2X, $P < 7\times10^{-4}$, Fisher's Exact Test).